Modeling of Power Supplies for Power Modulators with LTspice

Michael Giesselmann and **Vishwajit Roy**
Department of Electrical & Computer Engineering
Center for Pulsed Power & Power Electronics
Texas Tech University
Lubbock, Texas 79409, USA

ABSTRACT

This paper is showing simulations of power supplies for repetitive power modulators using LTspice. We are presenting power supplies with single-phase and three-phase AC input and the effects of the rectifier stages on AC input current waveforms in both cases. We are also presenting the resulting power factor including circuits for electronic power factor correction. LTspice models for electronic power factor correction using cycle-by-cycle switching as well as time-averaged models are presented. The time-averaged models replace the PWM (pulse width nodulation) switch with a transformer model with variable duty cycle. They are valid for a range of DC-DC converters. We are extending the time-averaged model for operation in continuous (CCM) and discontinuous (DCM) conduction mode and presenting results that show the fidelity of these models by comparison to cycle-by-cycle results. We are providing the detailed mathematical derivation for the DCM model expansion in the appendix. Time-averaged models do not have to keep track of thousands of steep switching transitions and can run orders of magnitude faster than cycle-by-cycle switch-mode models. Results using the time-averaged model are presented for a power supply with primary (wave-shaping) and cascaded secondary feedback control that regulates the output voltage of the converter.

Index Terms — **power electronics, power factor correction, time averaged models, feedback control, circuit simulation**

1 INTRODUCTION

POWER modulators for repetitive operation that are prominently featured at the bi-annual International Power Modulator and High Voltage Conference (IPMHVC) need power supplies that can deliver a high power DC intermediate voltage bus to power the actual modulator which is commonly creating high voltages (HV) in the range of 10's or 100's of kV [1,2]. The primary input source is typically 120– 240V single phase or 208– 500 V three phase AC. For power levels in the range of kW to 10's of kW or higher, the power supplies must adhere to current distortion limits outlined in IEEE standard 519-2014 [3]. Non-adherence to these standards will result in a low power factor because only the fundamental component of the input current creates real power since the supply voltage is a near perfect sinusoid.

The harmonic components are not providing real power but contribute to the RMS magnitude of the input current and create losses and disturbances in the power grid. This is true in particular in power supplies with single phase input. A single phase rectifier without a large buffer capacitor will have a DC ripple of 100 % amplitude and be unsuitable for a DC bus voltage for almost every application. However a large DC buffer capacitor sized to supply power for halve a cycle of the power frequency will be re-charged in a sharp spike around the peak of the supply voltage resulting in a very non-sinusoidal current with a large harmonic content and poor power factor. The novel contribution of this paper is to introduce the reader to the circuit simulation of power supplies for power modulators with LTspice [4]; a powerful design and analysis tool. We also present advanced time-averaged models for power supplies with low input harmonics and modeling of cascaded feedback loops.

2 BASIC AC RECTIFIER INPUT CIRCUITS

In this section, we will discuss typical AC rectifier circuits and their characteristics. We will show schematics with advanced use of hierarchical blocks with individual local parameters that are reusable building blocks for many examples in this paper and de-clutter the main schematic, which allows the reader to focus on essential topologies.

Manuscript received on 30 July 2018, in final form 4 January 2019, accepted 12 January 2019. Corresponding author: M. Giesselmann.

DOI: 10.1109/TDEI.2019.007721

2.1 SINGLE PHASE AC RECTIFIER

Figure 1 shows the topology of a basic AC front end for single phase voltage that is a using a full-bridge rectifier circuit and a large buffer capacitor laid out in LTspice. The full bridge rectifier is drawn so that it can be easily expanded to a three phase rectifier. The LTspice version of the generic Spice simulator is very useful for modeling power supplies and switch-mode power electronics circuits. In fact, Analog Devices supplies a large numbers of models for switch mode power conditioning devices for the code . However proper placement of the ground reference node and sophistication in the generation of control signals for power semiconductor switches are still important. Here we are putting a solid ground on the return of the AC input source. For stability, the negative rail of the DC bus (labeled Out-) is also grounded through a 1 MΩ resistor. To de-clutter the circuit, this resistor is located in the Pre-Charge circuit block, which is pre-charging the (floating) DC buffer capacitor to 150 V to ensure steady state conditions right after start-up. If the DC bus capacitor were solidly grounded, it could be initialized (pre-charged) using and .IC condition statement.

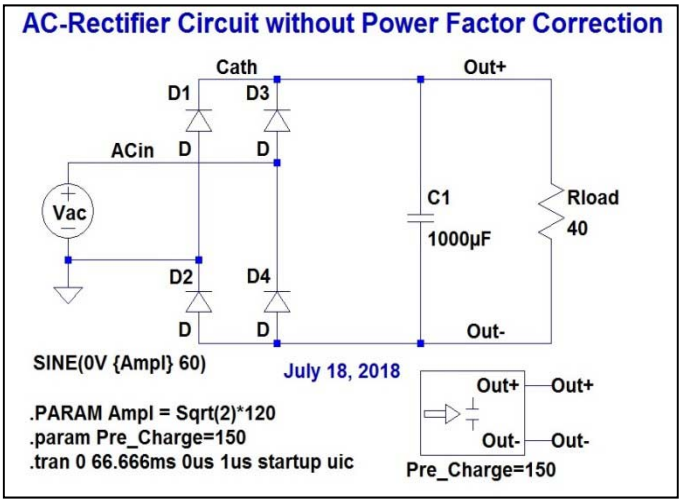

Figure 1. LTspice schematic of a basic single-phase rectifier circuit.

Double-clicking on the pre-charge circuit reveals the schematic for this pre-charge circuit which is shown in Figure 2. This hierarchical symbol was created with the schematics editor that is used to draw the schematics. It was saved as a symbol with the extension .asy. To define the functionality of the symbol, we created the associated sub-circuit shown in Figure 2 and saved it with the same name and an .asc extension. The sub-circuit contains a pre-charge voltage source "PreCharge1" and a switch that opens shortly after (1.8ms in this case) the start of the simulation. The pre-charge voltage source has a value of {Pre_Charge}, which is a local parameter that is associated with the hierarchical symbol and is passed to the voltage source.

Since the parameter is local, different values can be passed on to different instances of the pre-charge part, making it more versatile. A global parameter with the same name defines a default value.

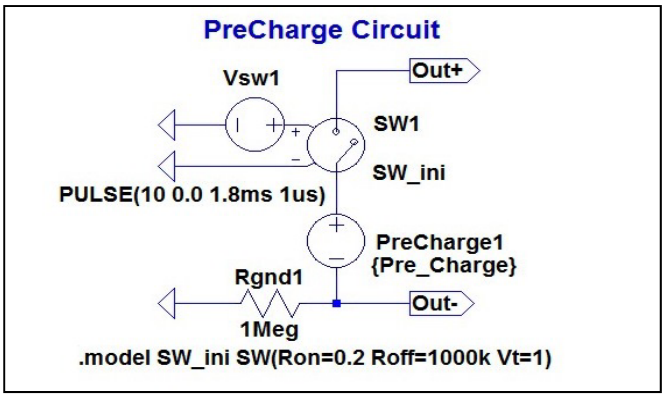

Figure 2. LTspice schematic of the sub-circuit associated with the Pre-Charge symbol. The Out+ and Out- interface ports connect to the equally named terminals of the associated symbol.

Figure 3 shows the result of the simulation of the single-phase rectifier circuit. In the upper pane, the trace of the DC output voltage is shown oscillating between 141 and 168 V resulting in 17 % ripple. In the lower pane the AC input current is shown with a peak of about 27 A.

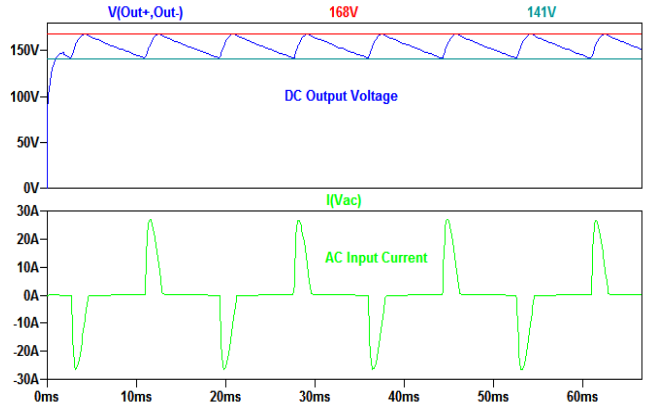

Figure 3. Typical waveforms of the single-phase rectifier circuit. The top trace shows the DC output voltage with 50V per tick mark. The bottom trace is the AC input current with 10A per tick mark and a 30A peak.

Figure 4 below shows a feature in the waveform viewer that shows the RMS value of the input current by selecting the trace and holding the Ctrl key and clicking the left mouse key.

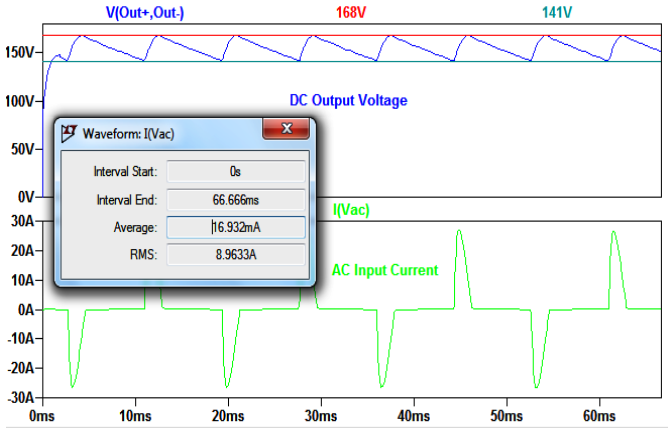

Figure 4. Using the waveform viewer to determine the RMS value of the AC input current. The indicated value is 8.9633 A.

Using the same technique we can determine the average and RMS DC output voltage to be 155 V. Using these values to calculate the output power into the 40 Ω load (600 W) and dividing by the apparent input power (product of RMS values of voltage (120 V) and current) we arrive at a very poor power factor of 56 %.

Figure 5 confirms that the input current waveform has a large number of strong harmonics that is out of compliance with IEEE 519-214 [3].

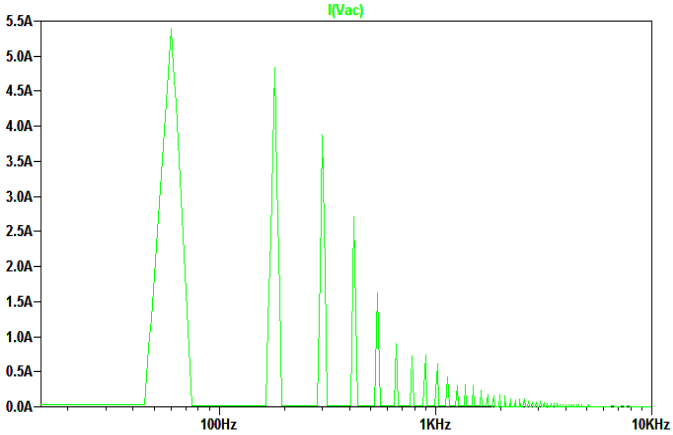

Figure 5. Frequency spectrum of the input current of the single-phase AC rectifier. Vertical scale: 0.5 A per tick mark, peak 5.5 A. Horizontal scale: Logarithmic, 100 Hz, 1 kHz, 10 kHz.

2.2 THREE-PHASE AC RECTIFIER

Using a three-phase input source creates a much better input waveform compared to a single-phase rectifier without any additional measures. The ripple of the DC voltage of a three-phase rectifier without any buffer capacitor is comparable with the ripple of the DC bus voltage of a single-phase rectifier with a large DC bus capacitor. In addition the DC-bus gets recharged at a rate of 6 times the power frequency. Figure 6 shows the LTspice schematic of such a circuit. Here the DC bus capacitor is just 5 µF instead of 1,000 µF.

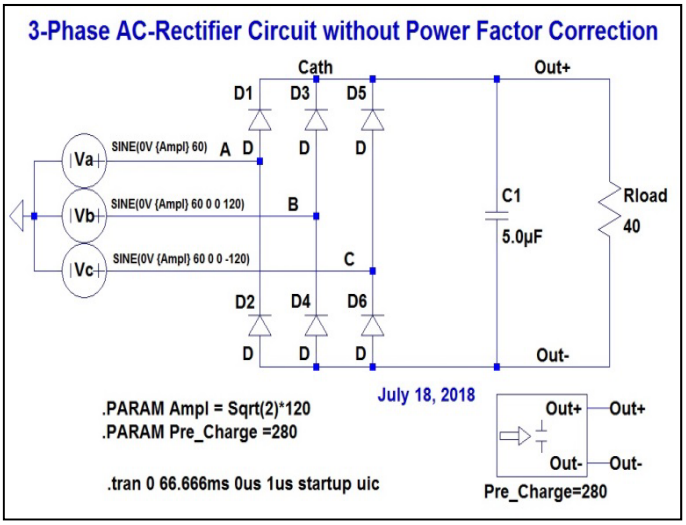

Figure 6. LTspice schematic of a three-phase rectifier circuit.

Figure 7 shows the typical waveforms of this circuit. The top trace represents the DC output voltage 292 and 252 V (14 % ripple). The average and RMS values are 279 volts. The lower trace represents the input current with an RMS value of 5.67 A. This results in a DC power of 1.95 kW into the load and a very respectable power factor of 95 %.

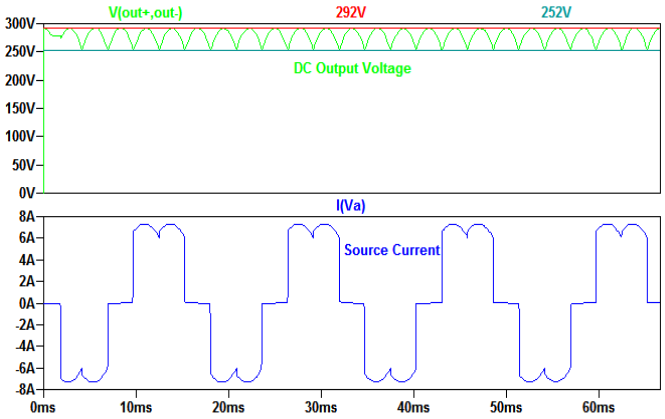

Figure 7. Typical waveforms of the three-phase rectifier circuit. The top trace shows the DC output voltage with 50V per tick mark and a top of 300V. The bottom trace is the AC input current with 2 A per tick mark and an 8 A max.

Figure 8 confirms that the spectrum of the input current of the three-phase rectifier has a much lower harmonics content with is consistent with the good power factor.

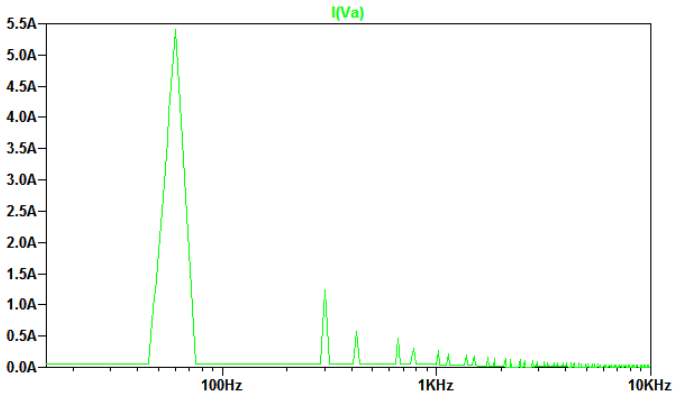

Figure 8. Frequency spectrum of the input current of the three-phase AC rectifier. Vertical scale: 0.5 A per tick mark, peak 5.5 A. Horizontal scale: Logarithmic, 100 Hz, 1 kHz, 10 kHz.

3 AC RECTIFIER CIRCUITS WITH POWER FACTOR CORRECTION

In order to reduce the harmonics of the input current drawn from the source and to improve the input power factor, especially for single-phase rectifiers, we are using a boost converter after the rectifier bridge to shape the input current to represent a rectified sinusoid. The boost converter is ideal for this since the current in the series input inductor is continuous and can be controlled to almost any shape by adjusting the duty cycle of the PWM switch [5]. Also the fact that the output voltage of a boost converter is higher than the input is

advantageous for repetitive Power Modulator applications that often feed high voltage loads. A high DC bus voltage can help the design by reducing the overall step-up ratio.

3.1 MODELS FOR BOOST CONVERTERS

In this section, we are examining models for Boost converters for use with LTspice. We are going to compare a conventional model for switch-mode operation of the boost converter as well as a model with a time-averaged switch [6]. We present a sub-circuit for the time-averaged switch that can be used for both continuous and discontinuous conduction mode. The advantage of a model with a time-averaged switch is that it can run much faster (by orders of magnitude) than the cycle-by-cycle switch-mode model since it can operate at a much larger time step [7]. In contrast, the cycle-by-cycle switch-mode model needs to operate at a small enough time-step to accurately follow each switch transition. As an example, for the simulation shown in Fig. 14 below, the execution time for the cycle-by-cycle switching model is 74 sec while the execution time for the time averaged model is only 2 sec. It should be noted that this simulation time advantage is for a short run of only 30 ms. In section 3.3 below we will demonstrate the use of a time - averaged model with cascaded feedback loops that runs for 800 ms. Here the fast run time of the time averaged model is very advantageous. This example will show that the time-averaged model is not a substitute for the conventional model but rather a complement especially for the design of feedback loops.

Figure 9 shows the LTspice schematic of the boost converters that are running side-by-side with identical component values to be able to validate the outputs of the cycle-by-cycle switch model and the time-averaged switch model. The converter with the time-averaged switch model is located on the lower part of the schematic. Each converter starts out in discontinuous conduction mode (DCM). At 2.5ms a switch adds additional load to each converter causing a transition to continuous conduction mode (CCM).

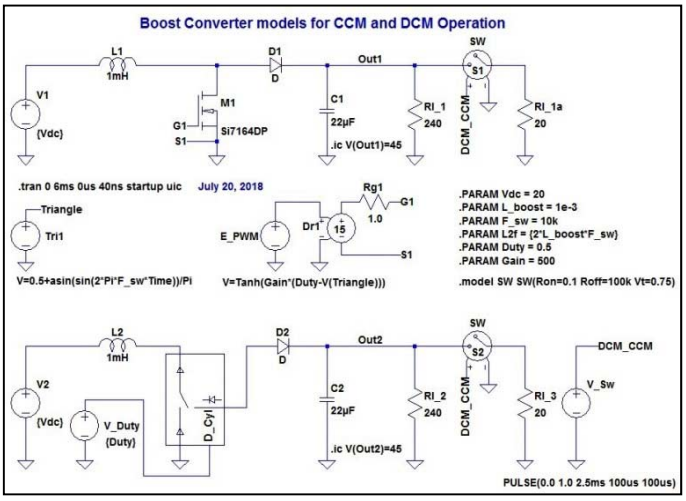

Figure 9. LTspice schematic of a Boost converter with cycle-by-cycle and time-average models operating in discontinuous conduction mode (DCM) and continuous conduction mode (CCM).

Figure 10 shows the sub-circuit of the time-averaged switch symbol in the lower circuit. The main circuit represents an ideal transformer with a turns-ratio which is controlled by the duty cycle [8]. Since the time-averaged switch can be used for a boost as well as a buck converter [6], the equations for the corrections for the duty cycle in DCM mode have been derived for a basic buck converter and are valid for this case. The controlled sources in the lower part of Figure 10 within the dashed rectangle sense and correct for proper operation in DCM mode. The equations are shown in the appendix and were derived in reference to [9]. For use of the time-averaged model in a buck converter the port labeled "Input" in Figure 10 is connected to the input voltage, whereas the port labeled "Out" is connected to the output LC filter of the buck converter.

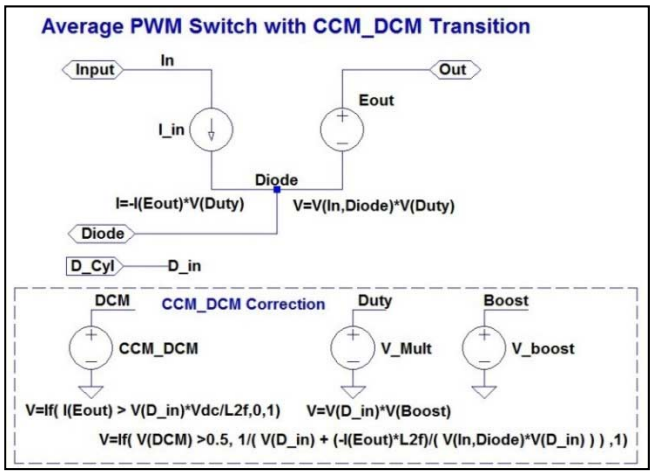

Figure 10. LTspice schematic of the sub-circuit of the time-averaged switch model for continuous conduction (CCM) and discontinuous conduction (DCM) mode.

Figure 11 shows the output of the simulation. It is very easy to see that the traces of the output voltage and the inductor current transition perfectly from DCM to CCM mode. The traces of the time-averaged model are exactly in the center of

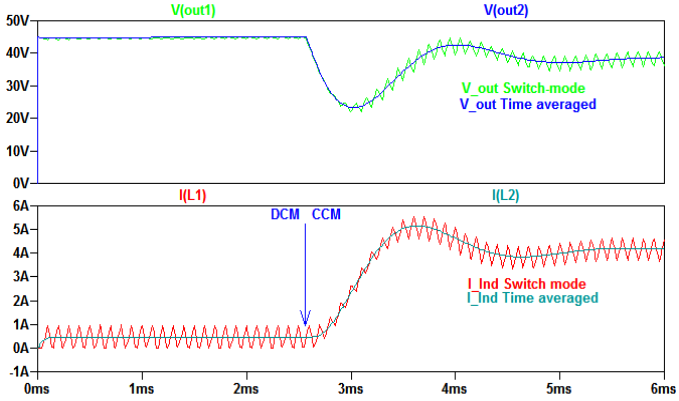

Figure 11. Output traces of a Boost converter with cycle-by-cycle and time-average models starting out in discontinuous conduction mode (DCM) and transitioning to continuous conduction mode (CCM). Top traces are the output voltages for both converters with a vertical scale of 50V max in 10V increments. Bottom traces are the inductor currents for both converters with a vertical scale of 6A with increments of 1.0A.

the waveforms of the cycle-by-cycle model. The amplitude of the excursions is determined by the percentage hysteresis of the PWM controller, which was chosen to be 5% in our case. If the hysteresis band would be smaller, resulting in a higher switching frequency, the cycle-by-cycle traces would have even less excursions to either side and be identical with the time-averaged traces.

3.2 BOOST CONVERTERS FOR POWER FACTOR CORRECTION

Figure 12 shows the schematic of the Boost converter which is used behind a full bridge rectifier to provide wave shaping of the AC input current input. To control the current a PWM controller is comparing the current in the inductor L1 with a sinusoidal reference and keeps the current within a hysteresis band around the reference [10]. This is achieved by turning the MOSFET M1 off if the current exceeds the upper boundary of the hysteresis band and turning the MOSFET back on when the current falls below the lower band. The width of the hysteresis band was set to 5 % for this example. The amplitude of the sinusoidal input current was chosen to be 10A. In a later example we are varying this amplitude in a secondary cascaded feedback loop to control the output voltage of the DC bus of the converter while maintaining perfectly sinusoidal current input shapes at all times.

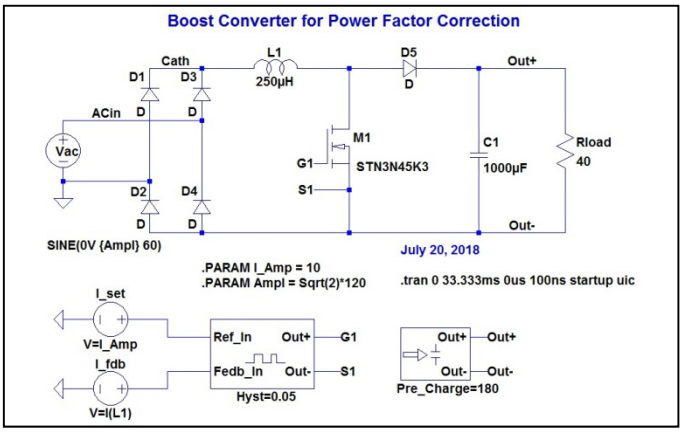

Figure 12. LTspice schematic of a Boost converter with cycle-by-cycle switching operating to control the wave-shape of the rectified current for power factor correction. The PWM controller is using Hysteresis control with a 5 % band around the reference.

Figure 13 shows the schematic of the hysteresis PWM controller. It provides a Gate voltage of ±15 V relative to the Source for the MOSFET M1. The positive voltage turns the MOSFET on while the negative voltage is used to quickly turn and keep it turned off. The voltage source Dr1 is boosting the voltage output from the PWM source PWM1 from ±1V to ±15V. The reference for the rectified sinewave is supplied by the voltage source Ref1. Ref2 adds or subtracts a hysteresis component of 0.05 (5 %) in this example by adding a fraction of the PWM voltage from PWM1 to Ref1 to arrive at Hyst_Ref. The source PWM1 compares this modified reference wave with the actual current level in the Boost inductor and derives a PWM switching signal using a soft comparator technique described in [6]. This technique provides a PWM signal well defines slope transitions using a hyperbolic tangent function. The low-pass filter Rg1, C1 provides a proper gate resistor and reduces the effect of the non-linear input capacitance of the MOSFET.

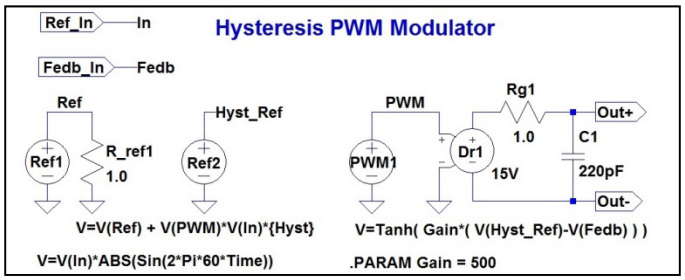

Figure 13. LTspice schematic of the sub-circuit of the Hysteresis PWM controller.

Figure 14 shows that the current in the inductor is almost perfectly sinusoidal. Using the results of the simulation, this circuit increases the Power factor to around 90 %.

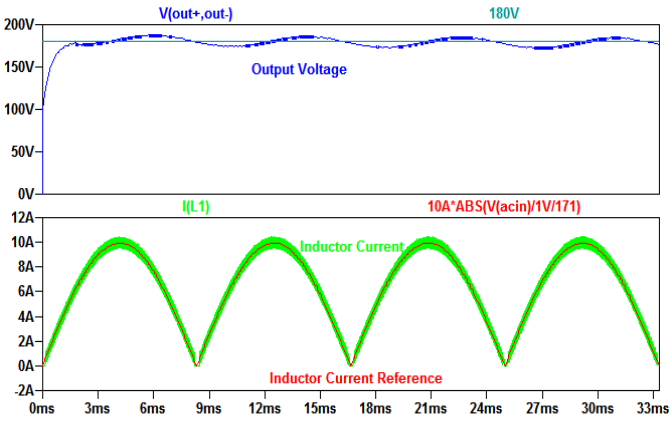

Figure 14. Output traces of the Boost converter shown in Figure 12. The top trace shows the output voltage 200 V max in 50 V increments. The bottom trace shows the inductor current with a vertical scale of 12 A max. with increments of 2.0 A.

3.3 POWER FACTOR CONTROL WITH TIME-AVERAGED BOOST CONTROLLER AND CASCADED FEEDBACK LOOPS.

Power supplies with active power factor correction need feedback control of the DC output voltage in addition to wave-shape control of the input current. To achieve this goal it is possible to keep the input current sinusoidal using a hysteresis controller in an inner current loop and controlling the peak of the sinusoidal input current in an outer feedback loop. Since a simulation of the regulation and performance of the outer loop will stretch over many cycles of the input voltage, the use of a boost converter model with a time-averaged switch is very important to avoid excessive simulation run times. Note that the in the example of Fig. 14 the run time to simulate 33ms (2 cycles of 60 Hz) was already 74 sec vs 2 sec for the time averaged model. Figure 15 shows the schematic of the setup

for a simulation with cascaded feedback loops with a time-averaged converter which is the premier application for this converter.

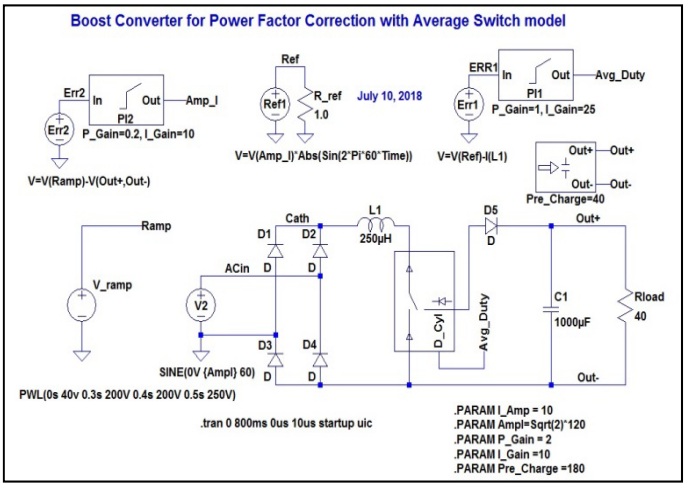

Figure 15. LTspice schematic of a Boost converter with time-averaged switching for active power factor correction with a cascaded feedback loop for output voltage control.

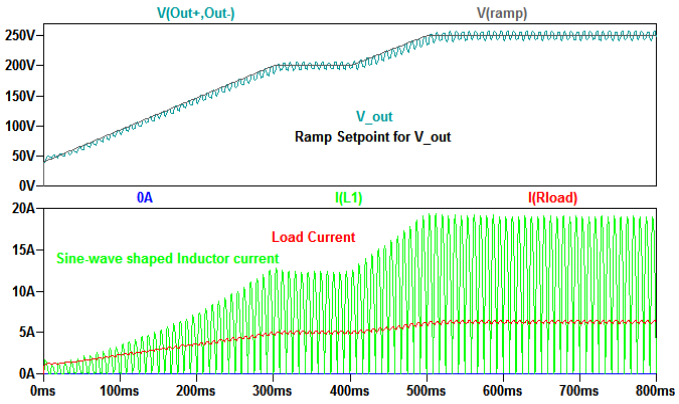

Figure 16. Output traces of the circuit setup shown in Figure 15. The top trace shows the output voltage in 50V increments along with the reference ramp. The bottom traces represent the sinusoidal input current with varying amplitude (green) as well as the average DC output current (red).The vertical scale has a max. value of 20 A with 5 A increments.

4 CONCLUSIONS

In this paper we have shown circuit simulation of power supplies for power modulators with LTspice. We demonstrated that LTspice is a powerful design and analysis tool for this application. We described cycle-by-cycle switching models as well as time-averaged models and validated the time averaged models. We believe that both types of models complement each other. We also presented advanced time-averaged models with automatic adjustment for DCM and CCM operation. The mathematical details are shown in the appendix in detail. We have shown that the main usefulness of the time-averaged modes is for modeling of cascaded feedback loops in power supplies with active controls for low input harmonics.

APPENDIX

In this appendix we derive the equation for the correction function of the time-averaged switch in DCM mode. We are writing an expression for the Voltage-Time integral across the Inductor of the Buck converter for DCM in steady state operation. During the on-time of the switch the difference between the input and the output voltage is across the inductor, whereas, during the off-time the output voltage is across the inductor with negative polarity. We define the following variables:

$V_d = V_{\_dc} input\ voltage$

$V_o = V_{\_output} voltage$

$D = Duty\ cycle$

$T_s = Switching\ Period, 1/Freq\_sw$

$\Delta_1 = Fraction\ of\ cycle\ for\ current\ decay\ to\ zero$

Ratio of Output to Input Voltage:

$$\frac{V_{oDCM}}{V_d} = \frac{D.T_s}{(D.T_s+\Delta_1.T_s)} = \frac{D}{(D+\Delta_1)} \qquad \frac{V_{oDCM}}{V_d} = \frac{D}{(D+\Delta_1)}$$

$$I_{L.peak} = \frac{V_o}{L}.\Delta_1.T_s \quad Peak\ inductor\ current$$

$$I_o = i_{L.peak}.\frac{D+\Delta_1}{2} \text{ Output current}$$

The average inductor current at the boundary of discontinuous operation is:

$$I_{LB} = \frac{1}{2}.I_{L.peak} = \frac{t_{on}}{2.L}.(V_d - V_o) = \frac{D.T_s}{2.L}.(V_d - V_o) = I_{oB}$$

Using $V_o = D.V_d$ we get: $I_{LB} = \frac{V_d.T_s}{2.L}.D.(1-D)$

The peak value is:

$$I_{LB.max} = \frac{V_d.T_s}{2.L}.\frac{1}{2}.\left(1-\frac{1}{2}\right) \qquad I_{LB.max} = \frac{1}{8}.V_d.\frac{T_s}{L}$$

Writing expression for the output current we get:

$$I_0 = \left(\frac{V_o}{L}.\Delta_1.T_s\right).\frac{D+\Delta_1}{2} = \left[\frac{\left[V_d.\frac{D}{D+\Delta_1}\right]}{L}.\Delta_1.T_s\right].\frac{D+\Delta_1}{2} =$$

$$\frac{1}{2}.T_s.\Delta_1.V_d.\frac{D}{L} = \frac{V_d.T_s}{2.L}.D.\Delta_1$$

Which leads us to an expression for Δ_1

$$I_0 = \frac{V_d.T_s}{2.L}.D.\Delta_1 = 4.I_{LB.max}.D.\Delta_1$$

$$I_0 = 4.I_{LB.max}.D.\Delta_1$$

$$\Delta_1 = \frac{1}{4}.\frac{I_o}{(I_{LB.max}.D)}$$

which leads us to the final expression for the voltage ratio in DCM mode:

$$\frac{V_{oDCM}}{V_d} = \frac{D}{(D+\Delta_1)} = \frac{D}{\left[D+\frac{1}{4}.\frac{I_o}{I_{LB.max}.D}\right]}$$

$$= \frac{D^2}{\left(D^2+\frac{1}{4}.\frac{I_o}{I_{LB.max}}\right)} = \frac{1}{1+\frac{2.L.f_s.I_o}{V_d.D^2}}$$

REFERENCES

[1] J.F. Tooker, P. Huynh, R.W, "Solid-State High Voltage Modulator With Output Control Utilizing Series-Connected IGBTs,"*IEEE Int. Power Modulator High Voltage Conf. (IPMHVC)*, 2014, pp. 27–30.

[2] C.W. Tipton, D. Ibitayo, D. Urciuoli, G.K. Ovrebo, "Development of a 15 kV bridge rectifier module using 4H-SiC junction-barrier schottky diodes," IEEE Trans. Dielectr. Electr. Insul., vol. 18, no. 4, pp. 1137–1142, 2011.

[3] Recommended Practice and Requirements for Harmonic Control in Electric Power Systems, IEEE Standard 519-2014, 2014-06-11.

[4] LTspice, Analog Devices, One Technology Way, P. O. Box 9106 Norwood, Massachusetts, 02062-9106, Available: http://www.analog.com/en/design-center/design-tools-and-calculators/ltspice-simulator.htm.

[5] Josef L. Smolenski, Gerard W. Christopher, John C. Wright, and Alfred E. Relation, "AC to DC Power Conversion circuit with low Harmonic Distortion," US Patent 5,019,952, May 28, 1991.

[6] M. G. Giesselmann, "Averaged and cycle by cycle switching models for Buck, Boost, Buck-Boost and Cuk converters with common averages witch model," *32nd Intersociety Energy Conversion Engineering Conference,(IECEC-97),* 1997, DOI: 10.1109/IECEC.1997.659210.

[7] H. Atighechi *et al*, "Dynamic average-value modeling of CIGRE HVDC benchmark system," IEEE Trans. Power Del., vol. 29, no. 5, pp. 2046–2054, 2014.

[8] Ned Mohan, *Electric Drives- An interactive Approach*, MNPERE, Minneapolis, 2003 edition, chapter 4.

[9] Ned Mohan, Tore M. Undeland, William P. Robbins, *Power Electronics, Converters, Applications, and Design*, John Wiley & Sons, Inc., 1989.

[10] R. W. Erickson, and D. Maksimovic, Fundamentals of power electronics, 2nd ed., Ed. New York: John Wiley, 1950, pp. 657–659.

Michael G. Giesselmann (M'86-SM'92) received his doctoral degree in Electrical Engineering in 1986 from the Technical University in Darmstadt, Germany. He holds the rank of Professor in the Department of Electrical and Computer Engineering at Texas Tech University. Dr. Giesselmann is a licensed Professional Engineer in Texas. Dr. Michael Giesselmann has been a principal faculty member and key researcher in the Pulsed Power Laboratory since 1986. Dr. Giesselmann worked on high power density designs for continuous operation at the 500 kW level for 60 kV DC as well as 13.8 kV AC 60 Hz output for ship borne & airborne applications.

Vishwajit Roy is currently a Ph.D student in the Department of Electrical and Computer Engineering at Texas Tech University. His current interests are Power electronics and renewable energy integration, Renewable energy applications, Smart grid, PMU data analysis and event detection.